Chapter 4 Elements of the 3D-Analysis of Deformation

4.1. General

Through analytical considerations it has been shown in the previous chapter that the 3D-Isoparametric and Lagrangian formulations of the Earth's surface deformations are ill-conditioned problems.

In this chapter, the conditioning of the problem is theoretically as well as numerically discussed in further detail using sensitivity analysis of least-squares solutions and simulated fields of deformation respectively. Simulated deformations provide theoretical results against which the computerized results should confirm. This procedure provides the valuable chance of checking the computer codes that have been developed for the practical application in this research. The spectral decomposition of the normal matrix provides an immediate insight into the conditioning of the problem. Nevertheless, identifying the parameters that are more sensitive to perturbations of input parameters requires a mathematical tool. A diagnosis technique has been forwarded in this research that can provide a detailed insight into the sensitivity of the deformation tensor elements to all possible perturbations of input parameters. Literally, the method is based on the possibility of indexing the deformation parameters with respect to each spectral value of the normal matrix. For this purpose, Principal Component Analysis (PCA), also known as Empirical Orthogonal Function Analysis, has been used. This is especially necessary for a deeper analysis of the Lagrangian formulation of the problem where our analytical consideration did not provide an insight into the conditioning of the problem, in the way it did for the Isoparametric approach.

When mathematical problems are to be numerically solved, they are classified to well-posed and ill-posed problems. A problem is considered to be well-posed if its solution exists, is unique and continuous under infinitesimal changes of inputs. A problem is ill-posed if either of these conditions is violated (Tikhonov and Arsenin, 1977). When the solution of a problem is not continuous under infinitesimal changes of inputs, the sensitivity of solution should be firstly analyzed. For discrete ill-posed problems, this is done through the analysis

of discrete Picard condition (Hansen, 1990). In this chapter, this condition will also be introduced. Moreover, it will be numerically verified for both the synthetic and real deformations of this study. Using simulation studies it will be shown that 3D-Lagrangian representation of the synthetic deformations are not sensitive to perturbations of input parameters.

The most two common sources for singularity and/or ill-posedness of a problem are its improper formulation and discretization of the problem (e.g. Aster et al., 2005). In these cases, singular and nearly singular problems should be numerically treated when there are no other alternatives for their reformulation and/or discretization other than the applied techniques. Regularization techniques are the necessary mathematical tools for treating ill-posed problems.

Truncated Singular Value Decomposition (TSVD) is proposed for regularizing the problem when 3D-representation of deformation is not continuous under infinitesimal changes of input parameters. Instead of the standard approach of L-curve analysis, optimum regularization parameters are estimated using the perturbation theory of TSVD. The efficiency of the method has been checked again for simulated deformations. To analyze the 3D-pattern of deformation in the test area, the method will be implemented to the corresponding GPS results.

4.2. Sensitivity of Least-Squares Solutions

The conditioning of a system and its impact on the system's solution have been defined and thoroughly analyzed in literatures about the accuracy and stability of numerical techniques (see for example: Dief, 1986; Jain et al., 2003; Björck, 1996; Higham, 2002). Traditionally, the problem is firstly analyzed for a consistent system of simultaneous equations.

Consider the linear system of equations:

$$\mathbf{A}\mathbf{x} = \mathbf{b}, \text{ where: } \mathbf{A} \in R^{n\times m}, \mathbf{x} \in R^{m\times 1} \ \& \ \mathbf{b} \in R^{n\times 1} \text{ and } n \geq m \tag{4.1}$$

In practice two types of error sources can contaminate the elements of the coefficient matrix **A** and vector **b**: 1) Observational errors and 2) Computational (rounding and chopping) er-

rors. Since a computer has a finite bit length, only a fixed number of digits are stored and used in computations. Therefore, even in exact decimal numbers, this gives rise to rounding and chopping errors (Mathews, 1999).

The analysis of the effect of perturbations given above on estimated parameters compared to the exact solution is the main aim in perturbation theory (Dief, 1986). The first question to be addressed is: Given the linear system (4.1), where now $\mathbf{A} \in R^{n\times n}$ and is nonsingular, what will be the effect to be seen on the solution $\mathbf{x}$ if we apply small perturbations $\Delta\mathbf{A}$ and $\Delta\mathbf{b}$ to $\mathbf{A}$ and $\mathbf{b}$ respectively:

Theorem 1.4.2: Let $\mathbf{A}$ be nonsingular and consider the consistent linear system $\mathbf{Ax} = \mathbf{b}$, the upper bound limit for the error in exact solution $\mathbf{x}$ due to perturbations $\Delta\mathbf{A}$ and $\Delta\mathbf{b}$ of $\mathbf{A}$ and $\mathbf{b}$ respectively in the perturbed linear system $\left(\mathbf{A}+\Delta\mathbf{A}\right)\tilde{\mathbf{x}} = \mathbf{b}+\Delta\mathbf{b}$, where $\tilde{\mathbf{x}}$ is the vector of perturbed unknown parameters, is:

$$\frac{\left\|\tilde{\mathbf{x}}-\mathbf{x}\right\|}{\left\|\mathbf{x}\right\|} \le \frac{k_2(\mathbf{A})}{\left(1-\left\|\mathbf{A}^{-1}\Delta\mathbf{A}\right\|\right)}\left[\frac{\left\|\Delta\mathbf{b}\right\|}{\left\|\mathbf{b}\right\|}+\frac{\left\|\Delta\mathbf{A}\right\|}{\left\|\mathbf{A}\right\|}\right] \tag{4.2}$$

where $k_2(\mathbf{A}) = \left\|\mathbf{A}\ \right\|_2\ \left\|\mathbf{A}^{-1}\right\|_2$ is called the *condition number* of $\mathbf{A}$.

Proof: Please refer to (Jain at al., 2003).

Corollary 1.4.2: Let $\mathbf{A}$ be a nonsingular and square matrix in the linear system $\mathbf{Ax} = \mathbf{b}$. The upper bound limit for the error in the exact solution $\mathbf{x}$ due to perturbation $\Delta\mathbf{b}$ in the perturbed linear system $\mathbf{A}\tilde{\mathbf{x}} = \mathbf{b}+\Delta\mathbf{b}$ is:

$$\frac{\left\|\tilde{\mathbf{x}}-\mathbf{x}\right\|}{\left\|\mathbf{x}\right\|} \le k_2(\mathbf{A})\frac{\left\|\Delta\mathbf{b}\right\|}{\left\|\mathbf{b}\right\|} \tag{4.3}$$

Proof: is immediately followed from Theorem 1.4.2, by putting $\Delta\mathbf{A} = \mathbf{O}$ where $\mathbf{O}$ is a *n*-by-*n* null matrix.

Equation (4.3) shows that in a system of linear equations, the condition number acts as a noise amplifier. In other words, the solution is not continuous under infinitesimal changes of inputs when $k_2(\mathbf{A})$ is large. The system of equations $\mathbf{Ax} = \mathbf{b}$ is said to be ill-conditioned If $k_2(\mathbf{A})$ is large. When $\|\ .\ \|$ is the spectral norm and $\mathbf{A}$ is real and symmetric, then

$$k_2(\mathbf{A}) = \left\|\mathbf{A}\right\|_2 \left\|\mathbf{A}^{-1}\right\|_2 = \frac{\lambda_{\max}}{\lambda_{\min}} \tag{4.4}$$

where $\lambda_{\max}$ and $\lambda_{\min}$ are the largest and smallest latent roots in modulus of **A**. For a rectangular matrix $\mathbf{A} \in R^{m\times n}$ where $m \geq n$ $\lambda_{\max}$ and $\lambda_{\min}$ are replaced by σ_1 and σ_r : the largest and smallest nonzero spectral values of **A** (Björck, 1996).

Similar to the linear system of equations above, the sensitivity of a least-squares solution can also be analyzed. The following theorem provides a norm-wise upper bound limit for the sensitivity of least-squares solution based on the perturbations $\Delta\mathbf{A}$ and $\Delta\mathbf{b}$ of the input parameters **A** and **b**.

Theorem 2.4.2: Let $\mathbf{A} \in R^{m\times n}$ $(m \geq n)$ and $\mathbf{A}+\Delta\mathbf{A}$ are both of full rank; and let: $\left\|\mathbf{b}-\mathbf{A}\mathbf{x}\right\|_2 = \min$, $\mathbf{r} = \mathbf{b}-\mathbf{A}\mathbf{x}$; $\left\|\left(\mathbf{b}+\Delta\mathbf{b}\right)-\left(\mathbf{A}+\Delta\mathbf{A}\right)\tilde{\mathbf{x}}\right\| = \min$, $\mathbf{s} = \mathbf{b}+\Delta\mathbf{b}-\left(\mathbf{A}+\Delta\mathbf{A}\right)\tilde{\mathbf{x}}$; $\left\|\Delta\mathbf{A}\right\|_2 \leq \varepsilon\left\|\mathbf{A}\right\|_2$, $\left\|\Delta\mathbf{b}\right\|_2 \leq \varepsilon\left\|\mathbf{b}\right\|_2$, then provided that $k_2(\mathbf{A})\varepsilon < 1$,

$$\frac{\left\|\mathbf{x}-\tilde{\mathbf{x}}\right\|}{\left\|\mathbf{x}\right\|} \leq \frac{k_2(\mathbf{A})\varepsilon}{1-k_2(\mathbf{A})\varepsilon}\left(2+\left(k_2\left(\mathbf{A}\right)+1\right)\frac{\left\|\mathbf{r}\right\|_2}{\left\|\mathbf{A}\right\|_2\left\|\mathbf{x}\right\|_2}\right) \tag{4.5}$$

Proof: Please refer to (Higham, 2002).

Corollary 2.4.2*:* Sensitivity of least squares solutions is measured by $k_2(\mathbf{A})$ when the residuals are small or zero and by $k_2(\mathbf{A})^2$ otherwise.

Proof: is straightforward form the theorem 2.4.2.

4.3. Sensitivity Analysis of Deformation Tensor

Through analytical derivations in previous chapter, it was shown that the network configuration plays a key role in the conditioning of the 3D-Isoparametric and Lagrangian representations of deformation. Except for some general conclusions that could be outlined there,

it was not possible to obtain a detailed insight into the sensitivity of the deformation tensor elements and the conditioning of the system. In the following subsections, using singular value decomposition and principal component analysis a diagnosis method will be forwarded for the sensitivity analysis of deformation tensor and a detailed study of the conditioning of the corresponding system of normal equations. To show the efficiency of the method, it will be tested using simulated deformations. Since for simulated deformations both theoretical strains and their numerical estimates are known, the relative and absolute accuracies of numerically estimated strain parameters can be assessed. The results of this analysis should conform to the diagnosis results when the diagnosis method of this chapter is implemented to simulated deformations.

4.3.1. Spectral Decomposition

Singular value decomposition (SVD) is a powerful mathematical tool for analyzing the conditioning of a problem. The interrelation of SVD and the conditioning of a system can be well understood through the following theorem known as the geometric SVD:

Theorem 1.4.3: Let $\mathbf{A} \in R^{n\times m}$ be a nonzero matrix with rank *r*. Then, there exists real numbers $\sigma_1 \geq \sigma_2 \geq ... \geq \sigma_r > 0$, an orthonormal basis $\{\mathbf{v}_1, \mathbf{v}_2, ..., \mathbf{v}_m\}$ which spans R^m and an orthonormal basis $\{\mathbf{u}_1, \mathbf{u}_2, ..., \mathbf{u}_n\}$ which spans R^n such that:

$$\mathbf{A}\mathbf{v}_i = \begin{cases} \sigma_i \mathbf{u}_i, & 1 \leq i \leq r \\ 0, & r+1 \leq i \leq m \end{cases}$$

$$\mathbf{A}^T \mathbf{u}_i = \begin{cases} \sigma_i \mathbf{v}_i, & 1 \leq i \leq r \\ 0, & r+1 \leq i \leq m \end{cases}$$

Base vectors $\{\mathbf{u}_1, \mathbf{u}_2, ..., \mathbf{u}_n\}$ and $\{\mathbf{v}_1, \mathbf{v}_2, ..., \mathbf{v}_m\}$ are called the left and the right singular vectors respectively.

Proof. Please refer to (Watkins, 2002, page 263).

Theorem 1.4.3 implies that any matrix $\mathbf{A} \in R^{n \times m}$ in the system (4.1) can be seen as a mapping tool that maps the parameter space P with dimension $\dim(P) = n$ to observation space L with dimension $\dim(L) = m$. If the parameter and observation spaces P and L are spanned by the basis $\{\mathbf{u}_1, \mathbf{u}_2, \ ..., \mathbf{u}_n\}$ and $\{\mathbf{v}_1, \mathbf{v}_2, \ ..., \mathbf{v}_m\}$ respectively, then the mapping between the two spaces is established by a set of positive numbers σ_i, $i = 1, 2, \ ..., r$, known as singular or spectral values.

Corollary 1.4.3: Each singular value of matrix **A** corresponds to a certain linear combination of the columns of **A** characterized by the elements of the right singular vector $\{\mathbf{v}_1, \mathbf{v}_2, \ ..., \mathbf{v}_m\}$.

Proof. The proof is straightforward from the geometric SVD theorem. From the geometric SVD theorem one can write $\|\mathbf{A}\mathbf{v}_i\|_2 = \sigma_i$, $i = 1, 2, \ ..., r$. Therefore, one or more small singular values σ_i imply that **A** is nearly rank deficient (ill-conditioned) and the vectors $\mathbf{v}_i$ associated with the small σ_i are the numerical null vectors of **A**.

The spectral decomposition of a matrix is normally illustrated by plotting the spectral values after arranging them in descending order. This representation is known as the spectral representation of a matrix. Analytically, the spectral decomposition of a matrix is well explained by the following theorem:

Theorem 2.4.3: Let $\mathbf{A} \in R^{m \times n}$ is a matrix of rank $p = \min(m, n)$, whose singular value decomposition is $\mathbf{A} = \mathbf{U}\mathbf{\Sigma}\mathbf{V}^T$. Matrix **A** can be written as the sum of *p* rank one matrices $\mathbf{E}_i$, $i = 1, ..., p$: $\mathbf{A} = \mathbf{E}_1 + \mathbf{E}_2 + ... + \mathbf{E}_p$ where, $\mathbf{E}_k = \sigma_k \mathbf{u}_k \mathbf{v}_k^T$ (Moler, 2004).

Unfortunately by spectral decomposition, it is not possible to analyze the interrelation of the unknown parameter and spectral values of a system. Partitioning the matrix **A** in the simultaneous system of equations (4.1) into specific sub-matrices when its elements can be classified to different groups can partially help remedy the problem. For example, the un-

known parameters in this study can be classified to horizontal (e_{xx}, e_{yy}, e_{xy}), vertical (e_{zz}, e_{xz}, e_{yz}) and rotational parameters (ω_x, ω_y, ω_z). Thereby, the spectral decomposition of each of the corresponding sub-matrices of these groups in the normal matrix can further clarify which parameters' group is degrading the conditioning of the system. Nevertheless, the analysis of the spectral forms of these sub-matrices can not exactly identify the parameters that are correlated more with each spectral value of the corresponding group. In other words, singular value decomposition can not be used for sensitivity analysis of the unknowns.

Using Principal Component Analysis (PCA), the diagnosis procedure outlined above can be further improved. It shall be shown in the next section that PCA can be used as a means for indexing the unknowns of a system with respect to its spectral values. This indexing process aids us to arrange the parameters of a system according to their interrelation with various singular values.

4.3.2. Principal Component Analysis

All the information concerning the precision of the least-squares estimate of a set of unknown parameters is included in the normal matrix whose inverse gives the variance-covariance matrix of the unknowns: $\mathbf{C}_{\hat{\mathbf{x}}} = \left(\mathbf{A}^T \mathbf{P} \mathbf{A}\right)^{-1}$. This information is geometrically visualized through multivariate confidence regions. For a certain risk level of α, multivariate confidence regions are characterized by (Vanicek and Krakiwsky, 1986):

$$\left(\mathbf{x} - \hat{\mathbf{x}}\right)^T \mathbf{C}_{\hat{\mathbf{x}}}^{-1} \left(\mathbf{x} - \hat{\mathbf{x}}\right) = \xi_{\lambda_u^2, 1-\alpha} \tag{4.6}$$

In two and three dimensions, this equation reduces to the well-known equations of error ellipse and error ellipsoid respectively. Visualizing confidence regions is a straightforward approach for the assessment of the sensitivity of estimated unknowns to the network configuration and observational errors. For larger systems where the number of unknowns is more than three, it will be too difficult to visualize such confidence regions. On the other hand, the

cross-correlation of the unknowns, hidden in the normal matrix, cannot be inferred from the geometrical representation of (4.6). Principal component analysis is a non-parametric mathematical tool by which all of the abovementioned information can be extracted from the covariance matrix of unknown parameters (Jackson, 2003).

The geodetic application of PCA has been limited to precision and sensitivity analysis of well-posed geodetic problems. The geometrical and statistical implications of various principal components makes it possible to efficiently analyze and visualize the local precision of geodetic networks when the number of unknown parameters is more than three. The implementation of principal component analysis to the Pelzer's geodetic theory of sensitivity analysis (Pelzer, 1976) has made it possible to analyze the sensitivity of the network in the direction of principal components and to define a threshold for detectable deformations (Leonhard and Niemeier, 1980; Niemeier, 1982).

In sensitivity analysis of the deformation tensor, in contrary to sensitivity and precision analysis of geodetic networks, the stability of the parameters of deformation is of interest. For this purpose, the sensitivity of these parameters to the network configuration and all possible types of input perturbations is analyzed. Moreover, the problem of the 3D-representation of deformation is an ill-conditioned problem. Therefore, we are no more concerned with the multivariate confidence regions. In addition to that, the sensitivities of all of the parameters to the perturbation of the inputs are of equal interest. The characteristics elaborated above show that the method to be forwarded for the sensitivity analysis of deformation tensor is a new and distinct approach to the application of PCA in deformation analysis.

From a theoretical point of view, PCA can be applied to any positive definite matrix **N** (Johnson and Wichern, 2002). This pre-requisite is also a characteristic feature of the normal matrix in all geodetic problems. The interrelation of PCA and SVD characterizes this mathematical apparatus as a valuable tool for analyzing the conditioning of a system. Especially, when analytical considerations fail to provide us a direct insight into the conditioning of a problem, such a numerical method is highly informative.

The application of PCA for the diagnosis of the stability and sensitivity of a system has been successfully implemented in this study. To explain the method, review of some theoretical aspects of principal component analysis is necessary. Therefore, the mathematical

background of this theory is firstly re-established through a few mathematical theorems. Then, using this mathematical background the method is explained and finally applied to simulated deformations.

4.3.2.1. Construction of Principal Components

Consider a vector of random variables $\mathbf{x} = \left[x_1, x_2, \ ..., x_p \right]^T$ with the covariance matrix $\mathbf{\Sigma}$. According to the propagation law of errors, any two linear combinations y_h and y_k of the random variables $x_1, x_2, \ ..., x_p$; i.e.: $y_h = \sum_{i=1}^{p} l_{ih} x_i$ and $y_k = \sum_{i=1}^{p} l_{ik} x_i$ have the variance $Var\left(y_n\right) = \mathbf{l}_n \mathbf{\Sigma l}^T$, n = h or k, and the covariance $Cov\left(y_k, y_h\right) = \mathbf{l}_h^T \mathbf{\Sigma l}_k$. By definition principal components are *uncorrelated* linear combinations $y_1, y_2, \ ..., y_p$ whose variances are as large as possible. Such uncorrelated linear combinations can be established through the following theorem:

Theorem 3.4.3: Consider the positive definite matrix $\mathbf{\Sigma}$ whose spectral decomposition is given by the eigenvalue-eigenvector pairs $\left(\lambda_i, \mathbf{e}_i\right)$, $i = 1, ..., p$, in which $\lambda_1 \geq \lambda_2 \geq \ ... \ \geq \lambda_p \geq 0$ is assumed. Then $\max_{\mathbf{z} \neq \mathbf{0}} \frac{\mathbf{z}^T \mathbf{\Sigma z}}{\mathbf{z}^T \mathbf{z}} = \lambda_1$ is attained when $\mathbf{z} = \mathbf{e}_1$ and $\max_{\mathbf{z} \perp \mathbf{e}_1, ..., \mathbf{e}_k} \frac{\mathbf{z}^T \mathbf{\Sigma z}}{\mathbf{z}^T \mathbf{z}} = \lambda_{k+1}$ is attained when $\mathbf{z} = \mathbf{e}_{k+1}$, $k = 1, 2, \ ..., p-1$.

Proof. Please refer to (Johnson and Wichern, 2002).

Corollary 2.4.3: Let $\mathbf{\Sigma}$ be the covariance matrix associated with the random vector $\mathbf{x} = \left[x_1, x_2, \ ..., x_p \right]^T$. Let $\mathbf{\Sigma}$ has the spectral decomposition $\left(\lambda_1, \mathbf{e}_1\right)$, $\left(\lambda_2, \mathbf{e}_2\right) \ldots \left(\lambda_p, \mathbf{e}_p\right)$ where for the singular values λ_i: $\lambda_1 \geq \lambda_2 \geq \ ... \ \geq \lambda_p \geq 0$ is assumed and

$\mathbf{e}_h = \left[e_{1h}, e_{2h}, \ ..., \ e_{ph} \right]^T$ denote orthonormal singular vectors in its spectral form. The h^{th} principal component is then given by:

$$y_h = \mathbf{e}_h^T \mathbf{x} = e_{1h} x_1 + e_{2h} x_2 + ... + e_{ph} x_p \tag{4.7a}$$

where for $h = 1, 2, ..., p$

$$Var\left(y_h\right) = \mathbf{e}_h^T \boldsymbol{\Sigma} \mathbf{e}_h = \lambda_h \tag{4.7b}$$

$$Cov\left(y_k, y_h\right) = \mathbf{e}_h^T \boldsymbol{\Sigma} \mathbf{e}_k = 0, \quad \text{when } h \neq k \tag{4.7c}$$

Proof: is straightforward from Theorem 3.4.3.

Corollary 3.4.3: If $y_h = \sum_{i=1}^{p} e_{ih} x_i$, $h = 1, ..., p$, are the principal components of the positive definite matrix $\boldsymbol{\Sigma}$, then the correlation coefficients of variables x_j and the principal components y_h are given by:

$$Cor\left(x_j, y_h\right) = \frac{e_{jh}\sqrt{\lambda_h}}{\sigma_j}, \ j, h = 1, 2, ..., p \tag{4.8}$$

Proof: Please see (Johnson and Wichern, 2002).

The analysis of these correlation coefficients can identify the parameters that are equally correlated with the total variance λ_h of the h^{th} principal component.

The theorems and corollaries above establish the mathematical framework of the diagnosis approach of this research. In this approach, instead of the covariance matrix the principal components of the normal matrix are set up. This is because when the normal matrix is badly conditioned the computation of the covariance matrix is problematic. For this purpose, the normal matrix is firstly expressed in its spectral form. The stability of the system can be visualized through the spectral representation of the normal matrix whose spectral values have been already computed. Then, using Equation (4.7a) the corresponding principal components are established. Each principal component organizes the random variables (deformation parameters) into separate groups. The correlation coefficients between the principal components and all unknown parameters are then estimated using Equation (4.8). Finally, the computed correlation coefficients are used for organizing the random variables of each group

according to their individual correlation with the corresponding spectral values in ascending order. For smaller singular values, random variables that have larger correlation coefficients with the corresponding principal components are highly sensitive to perturbation of the input parameters.

Theorem 2.4.3 also provides us a means for verifying the diagnosis result. According to this theorem, a general matrix can be approximated by the sum of a few rank one matrices. Approximations of different order can be set up for the inverse of the normal matrix by truncating its spectral form at different terms. The product of each approximate inverse to the normal matrix naturally deviates from the identity matrix. This deviation is a measure for the resolution of the elements in the approximate inverse matrices. If the diagnosis process is carefully done, the most biased parameter in the first order approximation of the inverse of the normal matrix should be the parameter(s) that is identified as the most sensitive one(s) in the diagnosis process. The same argument holds when approximations higher than one are set up for the inverse of the normal matrix by taking $p-2$ and $p-3$ rank one matrices according to the theorem 2.4.3.

4.3.3. Application to Synthetic Deformations

- **Simulated Deformations**

For simulation, a network with 10 stations is taken into consideration. This network consists of a central point SI01, and a set of surrounding points SI02 … SI10 that are located at different distances, ranging from 120 Km to 230 Km from the central point. The height differences between the central and surrounding points varies from 700 m in station SI06 to 1140 m in station SI08. The site positions have been chosen in such a way that the network configuration does not impose any rank deficiency during the computation of synthetic deformations. This configuration is shown in Figure 4.1. The network is subjected to hypothetical deformations that are characterized by the following analytical displacement field:

$$
\begin{aligned}
u &= (1.029808\times10^{-7})X - (3.360293\times10^{-7})Y - (4.421633\times10^{-6})Z \\
v &= (1.029808\times10^{-7})X - (3.360293\times10^{-7})Y - (4.421633\times10^{-6})Z \\
w &= (1.029808\times10^{-7})X - (3.360293\times10^{-7})Y - (4.421633\times10^{-6})Z
\end{aligned} \tag{4.9}
$$

The equations above characterize a deformation field that is composed of compression, dilation and shear, i.e. deformation in horizontal as well as vertical direction.

Using Equations above, synthetic deformations, which serve as *theoretical* values in this study, are computed through analytical differentiation of the displacement field. A computer code that is based on symbolic programming technique has been used. Simulated deformations are recomputed using the programs that have been developed for the Isoparametric and Lagrangian analysis of deformations in three-dimensions. Computed deformations are checked against theoretical values obtained from simulation. For this purpose, the relative errors of estimated parameters versus simulated ones are computed and analyzed. It is assumed that input parameters, i.e. the station coordinates, are free from any systematic and gross error. In addition to that, observational errors are assumed to be normally distributed. These assumptions are assured in the simulation process when the station coordinates and their variance-covariance matrices are produced. Sub-centimeter level of accuracy for horizontal coordinates and centimeter level of accuracy for the vertical coordinate are set up when variance-covariance matrices of the station coordinates are simulated.

Theoretical and numerical estimates of the synthetic deformations are compared in Figure 4.1. Arrows in red are the theoretical horizontal principal strains. Numerical results for estimated horizontal deformations are shown in blue. Vertical deformations are shown with double arrows in north south direction. Theoretical and numerical vertical deformations are illustrated in green and yellow respectively. Arrow pairs that are pointing to each other show compressions whereas arrow pairs that are pointing away show dilations.

In this simulation, the comparison of theoretical strains to their numerical estimate shows that maximum relative error is less than 1% in all estimated deformation parameters. Maximum relative error normally occurs on the e_{zz} and e_{xz} components of the strain tensor. It shall be shown in this chapter that for the configuration of the simulation network in this study, these parameters are more sensitive to the perturbation of input parameters than the others.

- **Diagnosis of Simulated Deformations**

To illustrate the method outlined above, the conditioning and sensitivity of the deformation parameters in the 3D-Isoparametric and Lagrangian representations of the synthetic deformations above have been analyzed. For both types of representations, the normal matrix $\mathbf{N} = \mathbf{A}^T \mathbf{P}\mathbf{A}$ has been firstly set up. Then using the theorem 1.4.3, normal matrices are expressed in spectral form. Figure 4.2 shows the spectral representation of normal matrices for the configuration of station SI01 as computation point and the other stations as contributing points. Spectral values are shown by solid circles in this figure. The last five spectral values are also shown as insets in semi-logarithmic axes.

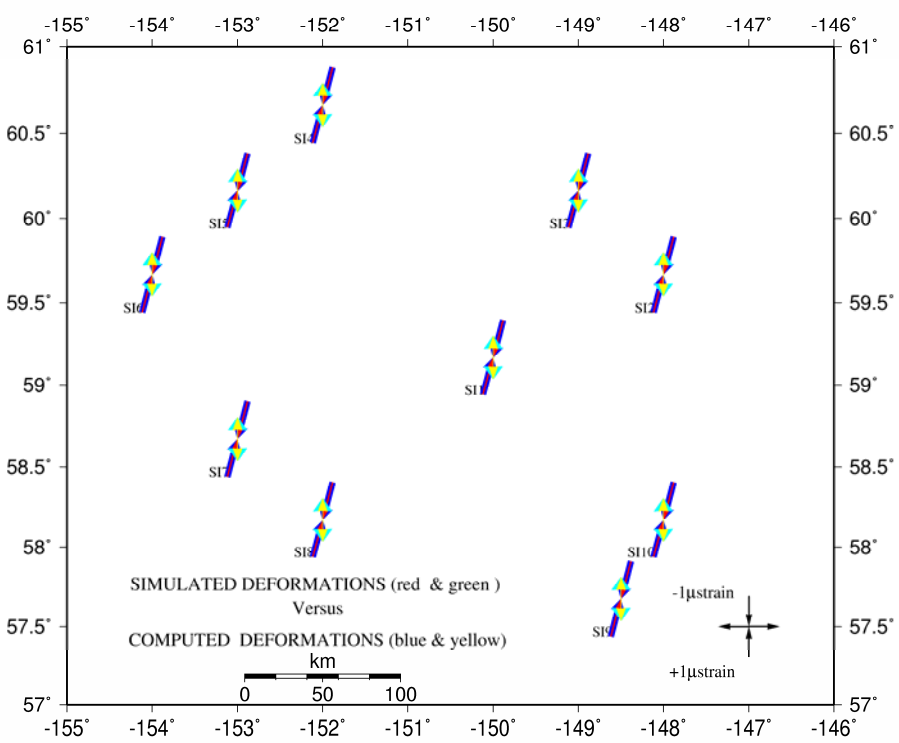

Figure 4.1: Theoretical 3D-principal synthetic strains versus 3D-principal strains that are computed using the Lagrangian approach to three-dimensional analysis of deformation

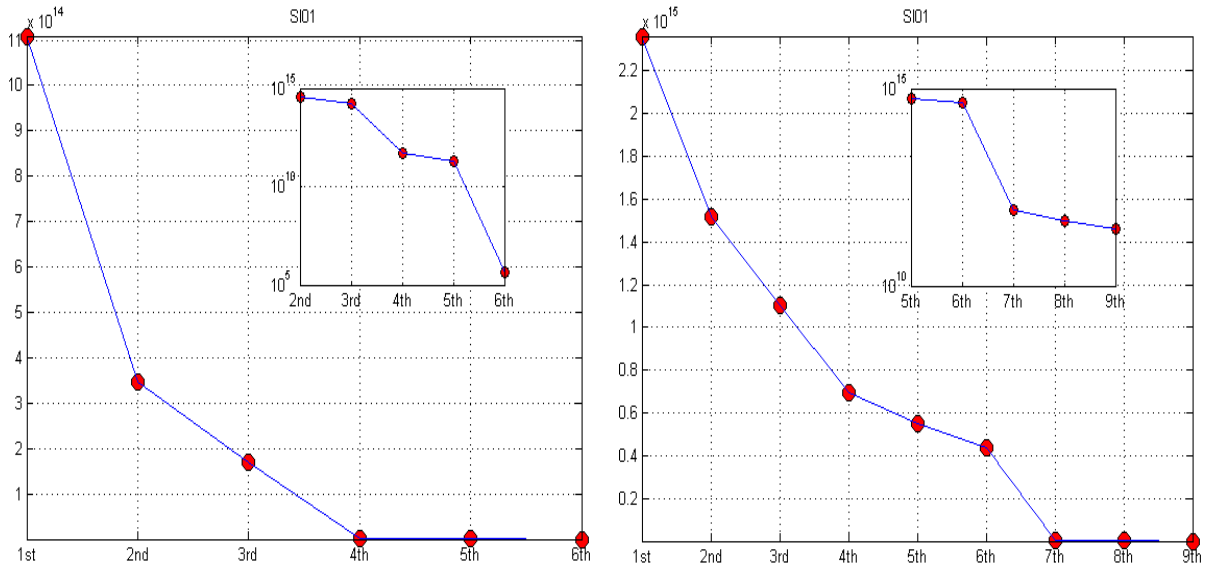

(a) (b)

Figure 4.2: Spectral decomposition of the normal matrix of station SI01 for Isoparametric (a) and Lagrangian (b) representations of the synthetic deformations.

Based on the formulae and the theory outlined above, principal components and their correlation coefficients with individual parameters of deformation are computed. Each principal component constructs a separate group. In each group, deformation parameters are arranged in ascending order according to the computed correlation coefficients in that group. Since each principal component corresponds to one singular value, parameters that are highly correlated with that principal component are more related to the corresponding singular value. For smaller singular values, such parameters identify the parameters that are more sensitive to the perturbation of input parameters. Figure 4.3 and Figure 4.4 illustrate the results of sensitivity analysis for the 3D-Isoparametric and Lagrangian deformation tensors of station SI01 (as computation point and the other stations as contributing points).

To check the sensitivity results, the resolution matrices of three successive approximations to the inverse of the normal matrix (see the subsection 4.3.2.1 for details) are also illustrated in Figure 4.3 and Figure 4.4. The comparison of the sensitivity results to the resolution matrices shows the feasibility of this method for a detailed sensitivity analysis of the deformation tensor in both the 3D-Isoparametric and Lagrangian representations of deformations. To make this comparison easier, during the construction of the design matrix **A**, the unknowns are grouped in horizontal, rotational and vertical parameters. More specifically, the

first three diagonal elements of the normal matrix in both 3D-Isoparametric and 3D-Lagrangian representations of the problem correspond to the parameters: e_{xx}, e_{yy}, e_{xy} and the last three diagonal elements to the vertical parameters: e_{zz}, e_{xz}, e_{yz}, respectively. The middle three diagonal elements of this matrix in Lagrangian formulation correspond to the rotational parameters: ω_x, ω_y, ω_z, respectively. Figures 4.3(a) and 4.4(a) illustrate the results of sensitivity analysis. Figures 4.3(b), 4.3(c), 4.3(d) and 4.4(b), 4.4(c), 4.4(d) are the resolution matrices for the three successive approximations of the normal matrices respectively. Each column in diagnosis matrices corresponds to one principal component. Principal components have been arranged in descending order. Therefore, the 1st and the last principal components correspond to the biggest and smallest singular values respectively. Since deformation parameters are arranged in ascending order, according to their correlation coefficient with the corresponding principal component, the lowermost parameters in each group are the most sensitive ones.

Diagonal cells of resolution matrices that are in dark brown posses the highest resolution where as diagonal cells that are in dark blue have the lowest resolution and therefore, are highly biased. For a perfect resolution matrix one expects dark brown diagonal cells versus dark blue off-diagonal ones. It is easily seen that with increasing the order of approximation in computing the inverse of normal matrices, the resolution of the most sensitive parameters are reduced. One can easily notice that for the configuration of station SI01 as computation point and the other stations as contributing points, in Isoparametric formulation of the problem the most sensitive parameters are e_{xz}, e_{zz} and e_{yz} respectively. For the same configuration, the most sensitive parameters in Lagrangian formulation of the problem are e_{yz}, e_{xy} and ω_z respectively.

The sensitivities of deformation parameters for 3D-representations of deformation have been also analyzed for the test area of this study. Appendix B is dedicated for the results of this analysis. Figures B1, B2 and B3 illustrate the sensitivity results of the 3D-Lagrangian representation of deformations in this area. Figures B4, B5 and B6 provide similar results for the 3D-Isoparametric approach.

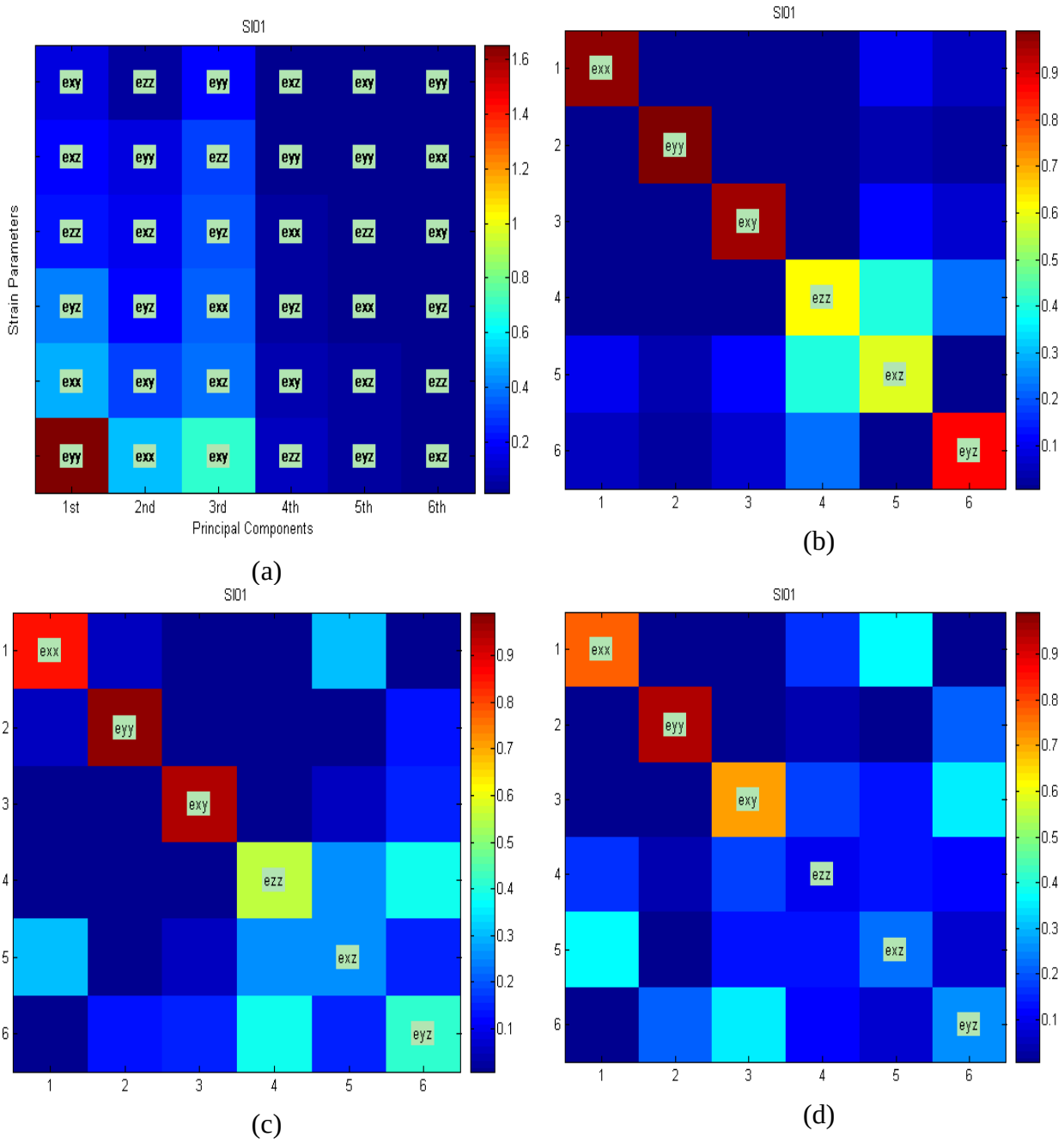

Figure 4.3: Sensitivity results and resolution matrices for the 3D-Isoparametric representation of deformation at station SI01.

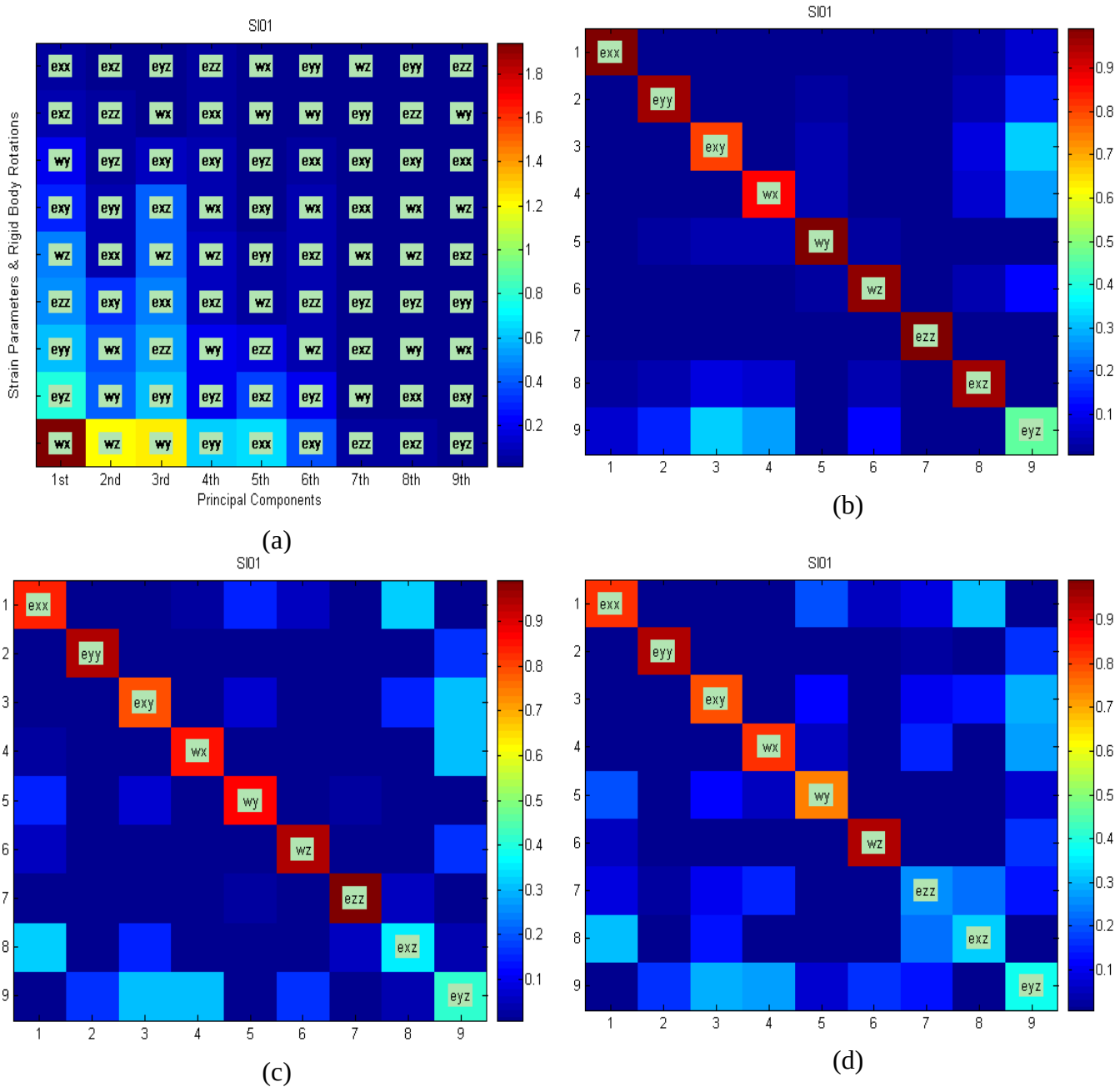

Figure 4.4: Sensitivity results and resolution matrices for the 3D-Lagrangian representation of deformation at station SI01.

4.4. Numerical Treatment of the 3D-Representation of Deformation

In the second section of this chapter it was shown that ill-conditioning is a property of the system of equations (it only depends on the design matrix **A**) and not the adopted numerical algorithm for solving the problem. Therefore, ill-conditioning cannot be simply treated by using a better numerical algorithm. Instead, either the float point arithmetic precision of computations should be improved or a better-conditioned system should be sought to replace the ill-conditioned problem (Aster et al., 2005). The new system might be based on reformulation of the problem or its replacement by a stable one which is literally based on the original system. In inversion theory, the latter is normally termed as *regularized* system.

Regularization techniques are the standard mathematical tools for treating discrete ill-posed problems. For this purpose, the instability of least-squares solutions is firstly analyzed. The instability of the least-squares solution in both the 3D-Isoparametric and Lagrangian representations of the synthetic and real deformations of this study will be analyzed using the discrete Picard condition (Hansen, 1990). By regularizing a problem its sensitivity to the input perturbations will be highly reduced. However, this will be at the cost of loosing the resolution on estimated parameters. Therefore, a tradeoff between the resolution and sensitivity of the system should be sought. This is the well-known tradeoff between stability and resolution. To overcome this problem it is also customary to look for an optimum regularization parameter. The analysis of the norm of residuals against the norm or the semi-norm of the solution, known as L-curve analysis, is one standard technique for estimating an optimum regularization parameter (see for example: Hansen, 1992, Aster et al., 2005).

An interesting aspect in many regularization techniques is that, if reasonable regularization parameters are used for each method, they (from a practical point of view) produce regularized solutions and corresponding residual vectors that are practically the same (Hansen, 1992). Therefore, once a reasonable solution is obtained by applying one regularization method it is not necessary to go for trying the other available techniques. Among different regularization techniques, truncated singular value decomposition (TSVD) is used for regularizing the problem of the 3D-representation of the Earth's surface crustal deformations. This is due to its simplicity for application and visualizing the process.

Regularization is a well-developed part of inversion theory but nevertheless is still subjected to further research. Since it is not the aim of this thesis to go for the theoretical consid-

erations of inversion techniques, only the practical aspects that are relevant to this study have been taken into consideration.

4.4.1. Discrete Picard Condition

The question that how well a regularized solution approximates an exact solution (regularization error) is an important aspect with regard to any regularization technique. In the analysis of regularization errors, perturbations of inputs are normally neglected. If $\mathbf{x}_t$ and $\mathbf{x}_k$ are the exact and regularized solutions of the discrete ill-posed problem:

$$\min_x \left\| \mathbf{A}\mathbf{x} - \mathbf{b} \right\|_2, \quad \mathbf{A} \in R^{m \times n}, \; m \geq n \tag{4.10}$$

$\left\| \mathbf{x}_t - \mathbf{x}_k \right\|_2$ is a measure for the regularization error. When truncated singular value decomposition is used for regularizing the problem, an upper bound limit for the regularization error ($\left\| \mathbf{x}_t - \mathbf{x}_k \right\|_2$) can be given by (Hansen, 1990):

$$\left\| \mathbf{x}_t - \mathbf{x}_k \right\|_2 \leq p^{\frac{1}{2}} \max_{1 \leq i \leq p-k} \left\{ \frac{\left| \mathbf{U}_{.,i}^T \mathbf{b} \right|}{\sigma_i} \right\} \tag{4.11}$$

Here σ_i, $i = 1, 2, .., p, p+1, ..., k$, are the singular values, vectors $\mathbf{U}_{.,i}$ are the corresponding left singular vectors in the spectral representation of matrix $\mathbf{A}$ and *k* is the total number of singular values with *p* nonzero values. Products: $\left| \mathbf{U}_{.,i}^T \mathbf{b} \right|$ are normally called Fourier coefficients. Equation (4.11) shows that smaller regularization error is expected to be present in the regularized solution, if on average the Fourier coefficients decay faster than the corresponding singular values. This property is known as the *discrete Picard condition*. The condition is numerically analyzed using the moving geometric mean:

$$\rho_i = \frac{\prod_{j=i-q}^{i+q} \left| \mathbf{U}_{.,i}^T \mathbf{b} \right|}{\sigma_t}, \quad i = q+1, ..., n-q \tag{4.12}$$

where $q < n-2$ is an integer. Since Equation (4.11) ignores the perturbation of input parameters, the discrete Picard condition is only a necessary condition for getting a good regularized solution.

The discrete Picard condition can also assess the instability of a least-squares solution when the corresponding system of normal equations has a large condition number. This interrelation can also be seen in Equation (4.11) by selecting $k = 0$. To clarify this argument the least-squares solution of the problem (4.10) has to be expressed in its spectral form. According to the geometric SVD theorem (see theorem 1.4.3), the matrix **A** in the least-squares problem (4.10) can be expressed as the product of orthonormal matrices $\mathbf{U} = [\mathbf{U}_{.,1}, \mathbf{U}_{.,2}, ..., \mathbf{U}_{.,m}] \in R^{m \times m}$, $\mathbf{V} = [\mathbf{V}_{.,1}, \mathbf{V}_{.,2}, ..., \mathbf{V}_{.,n}] \in R^{n \times n}$ and the diagonal matrix $\mathbf{\Sigma} = diag(\sigma_1, \sigma_2, ..., \sigma_n) \in R^{m \times n}$, where $\sigma_1 \geq \sigma_2 \geq ... \geq \sigma_p \geq \sigma_{p+1} = ... = \sigma_n = 0$, that is:

$$\mathbf{A} = \mathbf{U}\mathbf{\Sigma}\mathbf{V}^T \tag{4.13}$$

Substituting this expression in the maximum likelihood solution $\mathbf{x} = \left(\mathbf{A}^T\mathbf{A}\right)^{-1}\mathbf{A}^T\mathbf{b}$ gives:

$$\mathbf{x} = \left(\mathbf{V}^T\right)^{-1}\mathbf{\Sigma}^{-1}\left(\mathbf{\Sigma}^T\right)^{-1}\mathbf{V}^{-1}\mathbf{V}\mathbf{\Sigma}^T\mathbf{U}^T\mathbf{b} = \left(\mathbf{V}^T\right)^{-1}\mathbf{\Sigma}^{-1}\mathbf{U}^T\mathbf{b} \tag{4.14}$$

For the *p* non-zero singular values, Equation (4.14) takes the following form:

$$\mathbf{x} = \mathbf{V}\left[\frac{1}{\sigma_1}\mathbf{U}_{.,1}^T\mathbf{b} \quad \frac{1}{\sigma_2}\mathbf{U}_{.,2}^T\mathbf{b} \quad ... \quad \frac{1}{\sigma_p}\mathbf{U}_{.,p}^T\mathbf{b}\right]^t \tag{4.15}$$

In the presence of random noise, even if the true data were orthogonal to $\mathbf{U}_{.,i}s$, $\mathbf{U}_{.,i}^T\mathbf{b}$ is very likely to be non-zero. When these non-zero values are divided by small singular values and then multiplied by $\mathbf{V}_{.,i}$, an unstable solution is obtained unless the Fourier coefficients $\mathbf{U}_{.,i}^T\mathbf{b}$ decay faster than the corresponding singular values. Therefore, according to Equation (4.15) for a stable least-squares solution the discrete Picard condition is automatically ful-

filled. In other words, the discrete Picard condition is also a necessary condition to obtain a stable least-squares solution.

For the configuration of station SI01 and station SI03 as computation and the other stations as contributing points, the discrete Picard condition is shown in Figure 4.5 for the simultaneous system of normal equations in both 3D-Isoparametric and Lagrangian representations of synthetic deformations. As can be seen in Figure 4.5, discrete Picard condition is not fulfilled in the 3D-Isoparametric representation of deformation. This is due to the last singular value in the spectral decomposition of the normal matrix. For the 3D-Lagrangian representation of deformations, on average Fourier coefficients decay faster than the singular values. Since the discrete Picard condition is not valid for the 3D-Isoparametric representation of synthetic deformations, the maximum likelihood solution is not a stable and therefore, not a reliable solution for this problem. In contrast, for Lagrangian representation of the synthetic deformations, the discrete Picard condition is valid. Moreover, the analysis of the relative errors in estimated simulated deformations shows that the least-squares solution of the 3D-Lagrangian representation of deformations for the synthetic deformations is a stable solution.

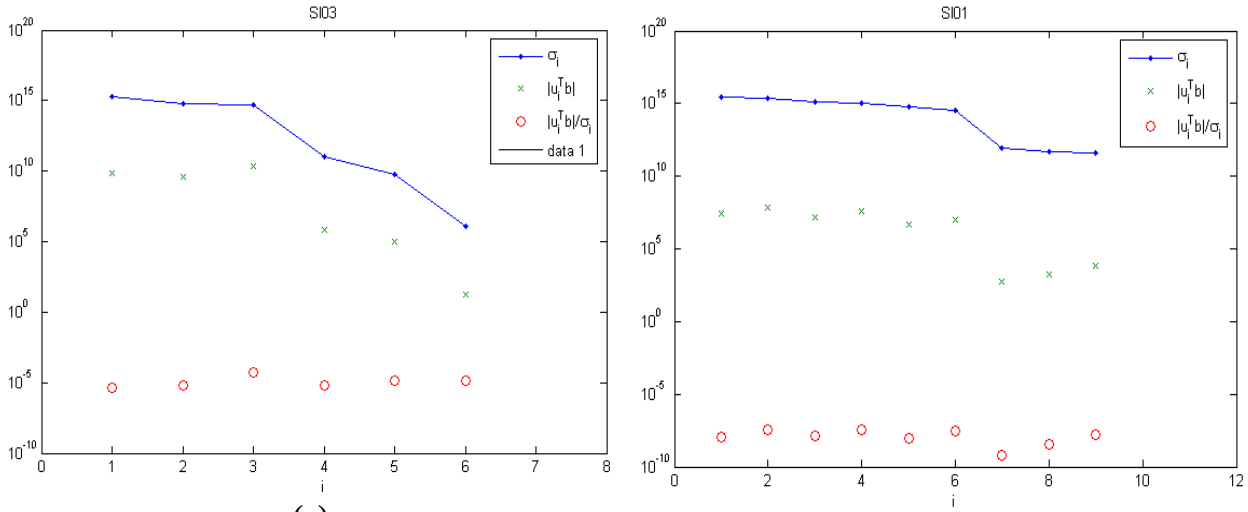

Figure 4.5: Discrete Picard condition for the 3D-Isoparametric (a) and 3D-Lagrangian (b) representations of synthetic deformations at stations SI01 and SI03. The Picard condition in not fulfilled for Isoparametric representation of deformation in station SI03 whereas for Lagrangian representation of deformation the condition in fulfilled in station SI01.

The discrete Picard condition has also been analyzed for 3D-representations of deformations in the test area of this study. Appendix C includes the results of this analysis. It can be easily seen in these results that for the configuration of the geodetic network stations in this area, both possible 3D-representations of deformation are sensitive to input noises and therefore, least-squares estimation of the corresponding (deformation) parameters is not reliable. Due to this, to improve the stability of solution it is necessary to go for regularization techniques.

4.4.2. Truncated Singular Value Decomposition (TSVD)

The application of Truncated Singular Value Decomposition (TSVD) for solving linear discrete ill-posed problems of type (4.10) can be traced back to Hanson (1971) and Varah (1973). Later, Hansen (1987) analyzed the problem in comparison to Tikhonov's (1963) and Philips' (1962) regularization technique. This study proved that the TSVD is a favorable alternative for the standard regularization technique of Tikhonov and Philips.

TSVD is literally based on the geometric SVD theorem (see theorem 1.4.3 and Equation 4.4.13). In this study $r = rank\,(\mathbf{A}) = n$ and there is no zero spectral value in the spectral decomposition of the normal matrix. Instead, the singular values asymptotically decay in such a way that the problem is ill-conditioned.

Similar to the other regularization techniques, the idea is to replace the ill-conditioned problem by a more stable one that is directly related to the main problem but, is less sensitive to the input perturbations. For this purpose, matrix $\mathbf{A}$ is replaced by $\mathbf{A}_k$ which is given by:

$$\mathbf{A}_k = \mathbf{U}\boldsymbol{\Sigma}_k\mathbf{V}^T,\quad \boldsymbol{\Sigma}_k = diag\,(\sigma_1,...,\sigma_k,0,...,0) \in R^{m\times n},\ k < n \tag{4.16}$$

$\mathbf{A}_k$ approximates $\mathbf{A}$ by substituting the last $n-k$ singular values by zero. Through this process the conditioning of the system improves to $k\left(\mathbf{A}_k\right) = \sigma_1/\sigma_k$ (Aster et al., 2005; Press et al., 1992). The regularized solution is finally given by:

$$\mathbf{x}_k = \mathbf{A}^{-1}\mathbf{b} \tag{4.17a}$$

$$\mathbf{A^{-1}} = \mathbf{V}\boldsymbol{\Sigma}_k^{-1}\mathbf{U}^T, \quad \boldsymbol{\Sigma}_k^{-1} = diag(\sigma_1^{-1},...,\sigma_k^{-1},0,...,0) \tag{4.17b}$$

As was mentioned earlier, the central point in any regularization technique is to find a compromise between the resolution of regularized solution and the stability of the system. This is achieved by finding an optimum regularization parameter. With regard to the truncated singular value decomposition, the number of singular values to reject plays the role of regularization parameter in comparison to the other regularization techniques like the method of Tikhonov and Philips. Perturbation theory of TSVD solution is a well-developed theory and is the key for finding an optimum regularization parameter in this technique. The following theorem of this theory is the key for finding an optimum regularization parameter for the TSVD solution (see for example: Hansen, 1987).

Theorem 1.4.4: For the perturbed TSVD solution $\tilde{\mathbf{x}}_k = \tilde{\mathbf{A}}_k\tilde{\mathbf{b}}$, where $\tilde{\mathbf{A}} = \mathbf{A} + \mathbf{E} = \tilde{\mathbf{U}}\tilde{\boldsymbol{\Sigma}}\tilde{\mathbf{V}}^T$ and $\tilde{\mathbf{b}} = \mathbf{b} + \mathbf{e}$, assuming that $\|\mathbf{E}\| < \sigma_k - \sigma_{k+1}$, the relative error of $\|\mathbf{A}_k^{-1}\|$ is bounded by:

$$\frac{\|\mathbf{A}_k^{-1} - \tilde{\mathbf{A}}_k^{-1}\|}{\|\mathbf{A}_k^{-1}\|} \le 3\frac{k_k}{(1-\eta_k)(1-\eta_k-\omega_k)}\frac{\|\mathbf{E}\|}{\|\mathbf{A}\|} \tag{4.18a}$$

where:

$$\begin{aligned} k_k &= \|\mathbf{A}\|\|\mathbf{A}_k^{-1}\| = \sigma_1/\sigma_k \\ \eta_k &= \|\mathbf{E}\|\|\mathbf{A}_k^{-1}\| = \|\mathbf{E}\|/\sigma_k = k_k\,\|\mathbf{E}\|/\|\mathbf{A}\| \\ \omega_k &= \|\mathbf{A} - \mathbf{A}_k\|\|\mathbf{A}_k^{-1}\| = \sigma_{k+1}/\sigma_k \end{aligned} \tag{4.18b}$$

Here, k_k is the condition number and ω_k is the size of the relative gap between the spectral values σ_k and σ_{k+1} in spectral representation of **A**.

Proof: Please refer to (Hansen, 1987).

The theorem shows for $\tilde{\mathbf{A}}_k^{-1}$ to be close to $\mathbf{A}_k^{-1}$, the relative gap ω_k should be small. This is because

$$3\frac{k_k}{(1-\eta_k)(1-\eta_k-\omega_k)}\frac{\|\mathbf{E}\|}{\|\mathbf{A}\|}=3\frac{\eta_k}{\omega_k}\left[\frac{1}{1-\eta_k-\omega_k}-\frac{1}{1-\eta_k}\right]$$

and therefore, for small ω_k the term in the square brackets tends to zero. A small ω_k corresponds to a well-determined gap between the singular values σ_k and σ_{k+1}. Therefore, if the SVD is to be successfully truncated at *k*, then there must be a well-determined gap between the spectral values σ_k and σ_{k+1}.

Taking this theorem into consideration, to find a tradeoff between the stability and resolution in a regularized TSVD solution, the accumulative relative gaps between each spectral value of the normal matrix and the last (smallest) one are analyzed. For this purpose, the cumulative relative gaps are plotted against the corresponding pair of spectral values. The 'well determined gap' of theorem 1.4.4 will correspond to the point in which a considerable change in the slope of this curve occurs. If a considerable change in the slope of the curve is observed between the spectral values σ_k and σ_p, where σ_p is the smallest nonzero singular value in spectral decomposition of the normal matrix, singular values $\sigma_{k+1},...,\ \sigma_p$ are ignored. The cumulative relative gaps for the 3D-Isoparametric representation of deformations at the two stations SI02 from the synthetic deformations of this study and KEN1 from the GPS crustal deformation array in the Kenai Peninsula are shown as insets in Figure 4.6. It is seen in this figure that at station KEN1 a remarkable change in the slope of the corresponding regularization curve occurs at the singular value pair (σ_7,σ_9). Therefore, to find a tradeoff between the stability and resolution of the regularized solution at this station the last two singular values should be rejected. Similar analysis for the synthetic deformations of this study at station SI02 shows that a remarkable change in the slope of regularization curve of this station occurs at the second pair of singular values, that is (σ_4,σ_6). Consequently, to get a reasonable regularized solution at this station two singular values should be rejected.

At the first glance, this method looks similar to the standard method of L-curve analysis, but the methods are basically different. This is because in the L-curve analysis technique the norm (or semi-norm) of solution is plotted and analyzed against the norm (or semi-norm) of residuals (Hansen, 1992).

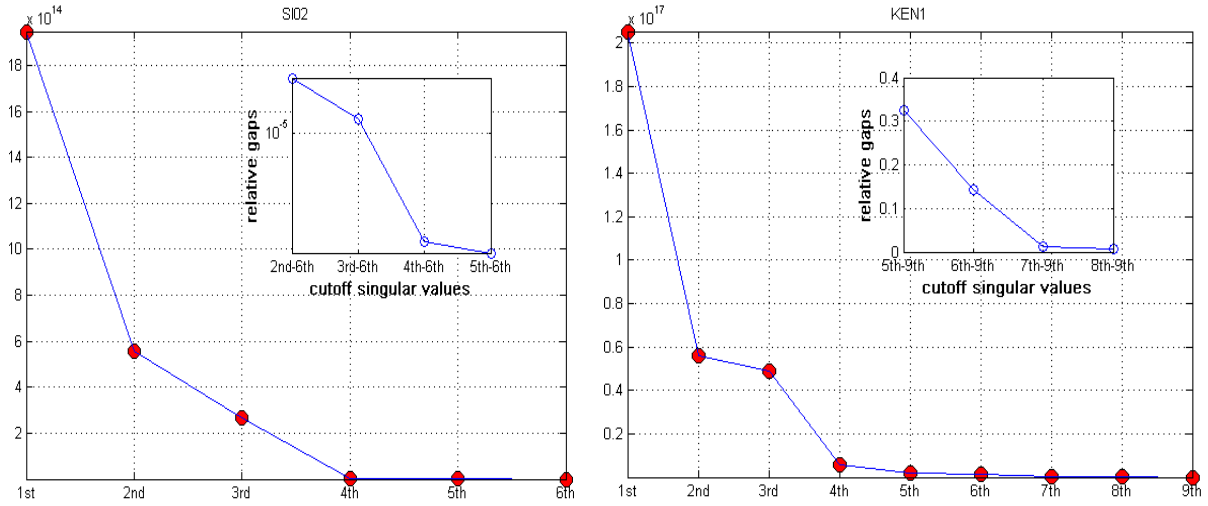

(a) (b)

Figure 4.6: Cutoff singular values for two stations SI02 from the network of synthetic deformations and KEN1 from the GPS deformation array in the Kenai Peninsula.

The efficiency of this method in finding an optimum regularized solution has been checked for the 3D-Isoparametric representation of the synthetic deformation mentioned above. For this purpose, the regularized solutions of the problem are computed using regularization parameters: $k = 6,\ 5,\ 4$ and 3 where for example, $k = 6$ corresponds to the non-regularized solution and $k = 5$ corresponds to the regularized solution in which the spectral representation of the normal matrix is truncated at its 5^{th} smallest singular value (5 singular values are retained). Then, the corresponding relative errors of regularized solutions are also computed using the theoretical strains. This comparison shows that for the synthetic deformations of this study, when $k = 5$ the TSVD solution obtains a minimum relative error. Moreover, computed relative gaps ω_k shows that a minimum gap also occurs between σ_5 and σ_6. The efficiency of this method for its application to real measurements will be shown in Chapter 7 where the computed pattern of deformation in the test area of this study is compared to the other available results on the deformations of this area.